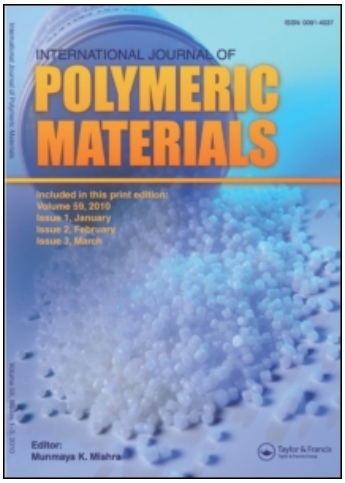

International Journal of Polymeric Materials
Publication details, including instructions for authors and subscription information:
http://www.informaworld.com/smpp/title~content=t713647664

Development and Electronic and Photonic Characteristics of Thiophene/Phenylene Co-Oligomers

Shu Hotta[a]; Toshifumi Katagiri[a]; Takeshi Yamao[a]; Koki Shimizu[b]; Hisao Yanagi[c]; Musubu Ichikawa[d]; Yoshio Taniguchi[d]
[a] Department of Macromolecular Science and Engineering, Graduate School of Science and Technology, Kyoto Institute of Technology, Kyoto, Japan [b] Isman J Corporation, Think Miraikobo, Kawasaki, Japan [c] Nara Institute of Science and Technology, Graduate School of Materials Science, Nara, Japan [d] Department of Functional Polymer Science, Faculty of Textile Science and Technology, Shinshu University, Ueda, Japan

To cite this Article Hotta, Shu , Katagiri, Toshifumi , Yamao, Takeshi , Shimizu, Koki , Yanagi, Hisao , Ichikawa, Musubu and Taniguchi, Yoshio(2008) 'Development and Electronic and Photonic Characteristics of Thiophene/Phenylene Co-Oligomers', International Journal of Polymeric Materials, 57: 5, 515 — 531
To link to this Article: DOI: 10.1080/00914030701816086
URL: http://dx.doi.org/10.1080/00914030701816086

International Journal of Polymeric Materials, 57:515–531, 2008

ISSN: 0091-4037 print/1563-535X online
DOI: 10.1080/00914030701816086

Taylor & Francis
Taylor & Francis Group

Development and Electronic and Photonic Characteristics of Thiophene/Phenylene Co-Oligomers

Shu Hotta
Toshifumi Katagiri
Takeshi Yamao
Department of Macromolecular Science and Engineering, Graduate School of Science and Technology, Kyoto Institute of Technology, Kyoto, Japan

Koki Shimizu
Isman J Corporation, Think Miraikobo, Kawasaki, Japan

Hisao Yanagi
Nara Institute of Science and Technology, Graduate School of Materials Science, Nara, Japan

Musubu Ichikawa
Yoshio Taniguchi
Department of Functional Polymer Science, Faculty of Textile Science and Technology, Shinshu University, Ueda, Japan

A novel class of organic semiconducting materials, thiophene/phenylene co-oligomers (TPCO), has been developed and synthesized. The materials are formed into crystals of high quality in a gas or liquid phase. These crystals exhibit unique optoelectronic properties such as a high carrier mobility and high quantum yield of emission. The transport properties have been studied on a device configuration of the field-effect transistor. The laser oscillation has definitively been observed for single crystals of the TPCO materials. In this article these optoelectronic features are presented and summarized.

Received 16 October 2007; in final form 29 October 2007.

The present study was partly supported by a Grant-in-Aid for Science Research in a Priority Area "Super-Hierarchical Structures" (No. 17067009) from the Ministry of Education, Culture, Sports, Science and Technology, Japan.

Address correspondence to Shu Hotta, Department of Macromolecular Science, Kyoto Institute of Technology, Matsugasaki, Sakyo-Ku, Kyoto 606-8585, Japan. E-mail: hotta@kit.ac.jp

Keywords: carrier mobility, field-effect transistor, laser oscillation, optoelectronic properties, organic semiconducting materials, quantum yield of emission, thiophene/phenylene co-oligomers (TPCO)

INTRODUCTION

Organic semiconducting materials have been drawing increasing attention for the last several decades thanks to their excellent optoelectronic properties. Many organic semiconductors are currently being studied both from a fundamental standpoint of materials science and with a view to applying those materials in optoelectronic devices. Of these organic semiconducting materials, conjugated molecules and polymers have large potential and a wide class of these materials has been proposed and developed. The integrated features regarding optics and electronics make these materials very attractive and promising. In particular, thiophene-based and phenylene-based materials (e.g., polythiophenes, oligothiophenes, polyphenylenes, and oligophenylenes) are most widely investigated among the conjugated molecular materials at this date [1,2]. It is therefore natural that one is stimulated to develop materials in which both thiophene and phenylene are hybridized at the molecular level, with the expectation that excellent transport and emission properties can be compatible.

The novel materials, thiophene/phenylene co-oligomers [3] (see Figure 1 for the structural formulae of several compounds), are characterized by the following aspects in light of the molecular and crystal design: (i) Various molecular shapes, e.g., bent, zigzag, pseudo-straight, etc., are readily accessible. These variations are brought forth by appropriately arranging the *pentagonal* thiophenes and *hexagonal* phenylenes in the molecule. (ii) Nonstraight molecules produce peculiar crystallographic structures where the molecular long axes stand (nearly) upright against the bottom crystal face. Those structures are responsible for interesting electronic and photonic characteristics of the TPCOs, such as high carrier mobility and spectrally narrowed emissions (SNEs) that are associated with high emission quantum yield of the crystals.

With these characteristics as a background, we summarize in the present review the synthesis and development of the TPCO materials. These TPCO materials are formed into crystals by various techniques and their electronic and photonic characteristics are investigated. The charge transport feature was investigated on the field-effect transistor (FET) configurations.

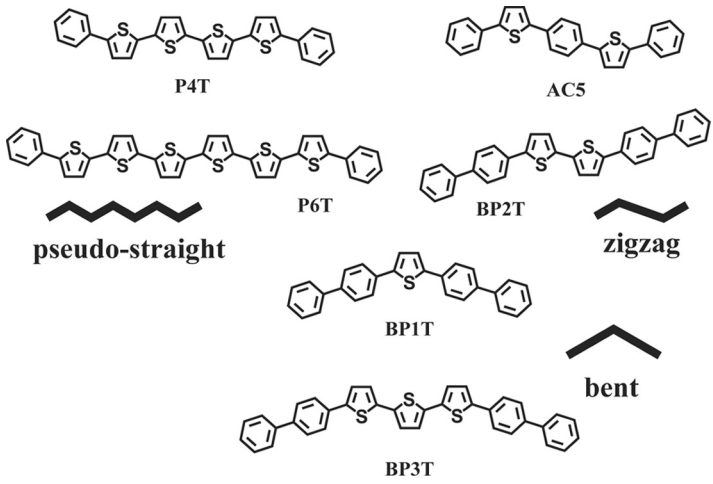

FIGURE 1 Several examples of thiophene/phenylene co-oligomers (TPCOs) and their various molecular shapes (pseudo-straight, zigzag, bent, etc.).

MATERIALS

The TPCO materials dealt with in the present study were synthesized via organic chemical routes mostly on the basis of Grignard coupling [4], Suzuki coupling [5], or Negishi coupling [6]. The overall synthetic strategy is shown in Figure 2 [3e], where (a) three blocks or (b) two blocks are joined so as to be the target compounds. In case the molecules are substituted with functional groups, they can be introduced before joining the blocks (Figure 2). The materials as synthesized were recrystallized from suitable solvents, higher molecular-weight materials exhibiting metallic luster after being recrystallized. A few examples of the synthetic routes are depicted in Figures 3 [3d] and 4 [3e].

The resulting compounds are sparingly soluble at room temperature in any organic solvent, when the number of aromatic rings (i.e. thiophenes and phenylenes) constituting the compounds is equal to five or more. In that case, however, the compounds can further be processed into thin films, e.g., via vacuum evaporation, and used for making the thin-film devices. To achieve enhanced electronic and photonic properties with the TPCOs we need large crystals and aligned materials of high quality. To this end, the crystals are grown as flakes by the sublimation of the TPCO materials either inside a sealed glass apparatus [7] or under inert gas flow [8]. Alternatively the materials are epitaxially formed on the KCl surface into needle

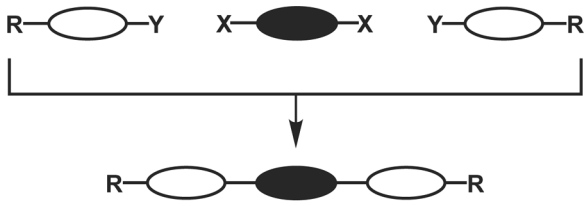

X = Br [ZnCl]; Y = $B(OH)_2$ [Br, I];
R = $(CH_2)_3CH_3$, OCH_3, CN, CF_3.

(a)

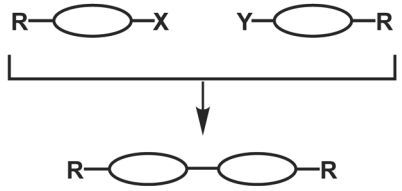

X = Br; Y = ZnCl;
R = $(CH_2)_5CH_3$, OCH_3, CF_3.

(b)

FIGURE 2 Synthetic strategy of the TPCO materials. Reproduced with permission from Katagiri, T., Ota, S., Ohira, T., Yamao, T., and Hotta, S., "Synthesis of thiophene/phenylene co-oligomers. V. Functionalization at molecular terminals toward optoelectronic device applications," *Journal of Heterocyclic Chemistry*, *44*, 853 (**2007**) [3e].

crystals or aligned thin films [9]. We carried out the crystal analyses with several of the TPCO materials [10].

As an option we have developed a novel method of making the organic crystals. This is characterized by the direct formation of thin single crystals on a substrate in a specially designed growth apparatus containing the TPCO solution [11]. The apparatus is equipped with a radiator that can release heat from the solution to the atmosphere to locally cool the substrate (in thermal contact with the radiator) and to keep its temperature lower than that of the surrounding solution. This allows thin crystals of well-defined polygons (e.g., hexagons, lozenges, swords) to grow directly on the substrate. The aforementioned crystals grown either in gas phase or liquid phase are potentially useful for semiconductor device applications.

The overall motif for the TPCO crystals is characterized by the "herringbone" structure [12] laterally spreading in parallel with the

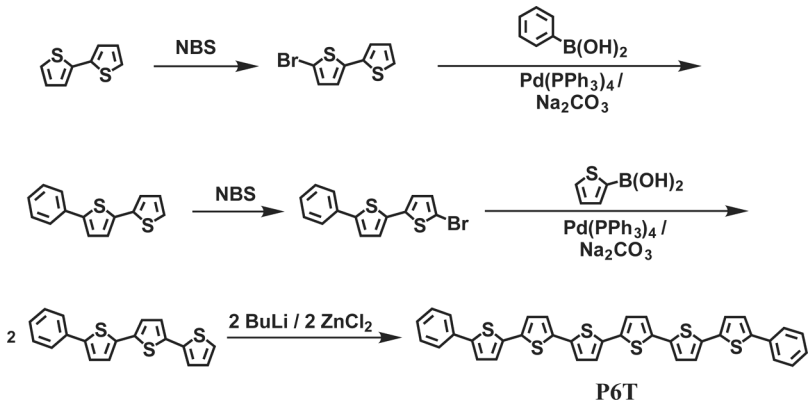

FIGURE 3 Synthetic scheme of P6T. Reproduced with permission from Hotta, S. and Katagiri, T., "Synthesis of thiophene/phenylene co-oligomers. IV. 6- to 8-Ring molecules," *Journal of Heterocyclic Chemistry*, **2003**, *40(Sep–Oct)*, 845–850 [3d].

bottom crystal face. The strong face-to-face π-π interaction among the molecules is responsible for this structure. A further feature is that the molecular long axes stand upright against the bottom crystal face. The angle between the molecular axis and the normal to the bottom plane is at most a few degrees [10b]. This unique feature is essentially pertinent to the novel photonic properties (vide infra). As typical examples we show in Figures 5 and 6 the crystal structures of BP2T

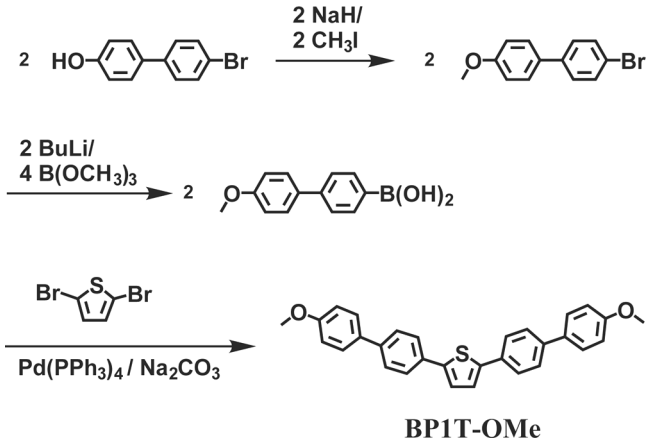

FIGURE 4 Synthetic scheme of BP1T-OMe. Reproduced with permission from *Journal of Heterocyclic Chemistry*, **2007**, *44(Jul–Aug)*, 853–862 [3e].

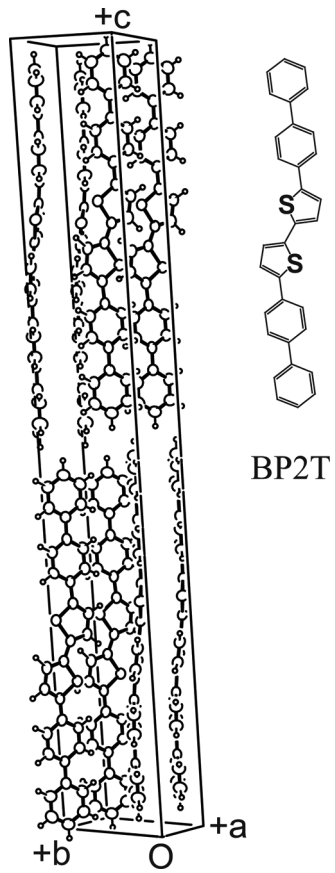

FIGURE 5 Crystal structure of BP2T [10b]. The inset molecule conforms to the upper right one in the crystal in both size and orientation.

and BP3T, respectively [10b]. In the case of BP1T-OMe the said angle is exactly 0° imposed from the symmetry requirement [10c].

ELECTRONIC PROPERTIES AND DEVICE APPLICATIONS

Figure 7 shows a schematic diagram of a FET device structure based on an organic semiconductor crystal. Ichikawa et al. [13] made the FET devices using the needle crystals of BP2T (see Figure 1). The needle crystals were grown on top of the KCl substrate and transferred onto a SiO_2/Si substrate by a wet transfer method [14]. The Si substrate works as a gate electrode. The 50-nm-thick gold electrodes as source and drain contacts were thermally evaporated on the

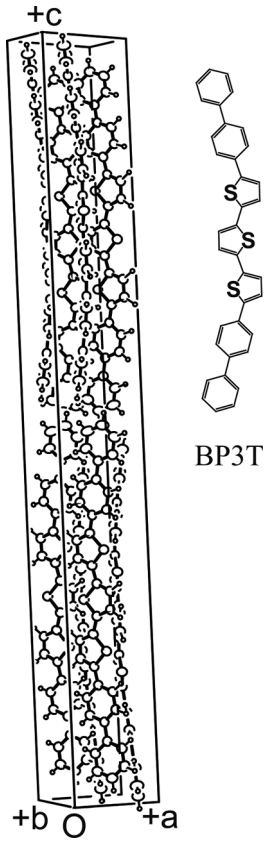

FIGURE 6 Crystal structure of BP3T [10b]. The inset molecule conforms to the upper right one in the crystal in both size and orientation.

BP2T crystals (see Figures 8 and 9) [13]. The channel length of the FET was 25 μm and the "effective" channel width (W_{eff}) was estimated with a digital microscope from the summed width of the needle crystals of the device (Figures 8 and 9).

Figure 10 [13] shows a set of drain current I_{d} vs. source-drain voltage V_{d} curves for various source-gate voltages V_{g} of the epitaxially grown BP2T FET at room temperature. The device operates in a p-channel accumulation regime. The field-effect mobility μ_{FET} was estimated from the saturation drain current in the pinch-off regime, $I_{\text{d,sat}}$, as follows [15]:

$$I_{\text{d,sat}} = \frac{W_{\text{eff}}}{2L} C_{\text{i}} \mu_{\text{FET}} (V_{\text{g}} - V_{\text{t}})^2, \tag{1}$$

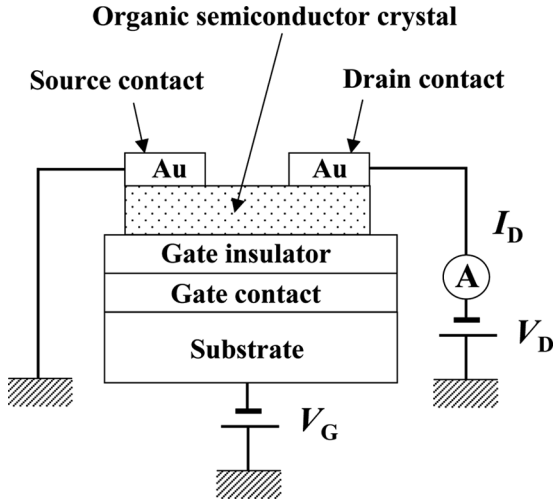

FIGURE 7 Schematic device configuration of a field-effect transistor using an organic thin crystal.

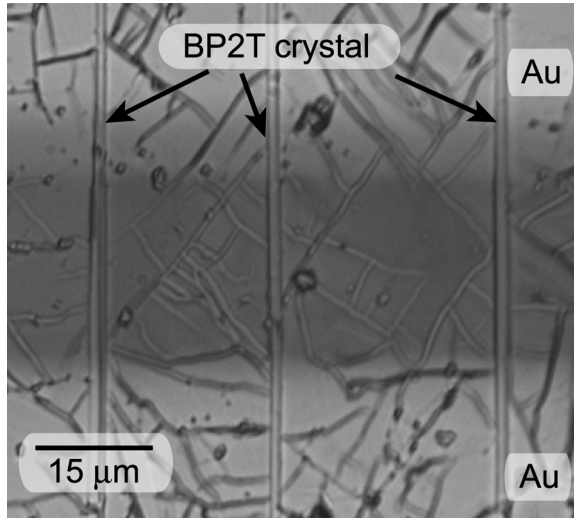

FIGURE 8 Optical micrograph of the FET device using the needle crystals of BP2T. Ichikawa, M., Yanagi, H., Shimizu, Y., Hotta, S., Suganuma, N., Koyama, T., and Taniguchi, Y., "Organic field-effect transistors made of epitaxially grown crystals of a thiophene/phenylene co-oligomer," *Adv. Mater.*, **14(18)**, 1272–1275 (2002). Copyright Wiley-VCH Verlag GmbH & Co. KGaA. Reproduced with permission from Ref. [13].

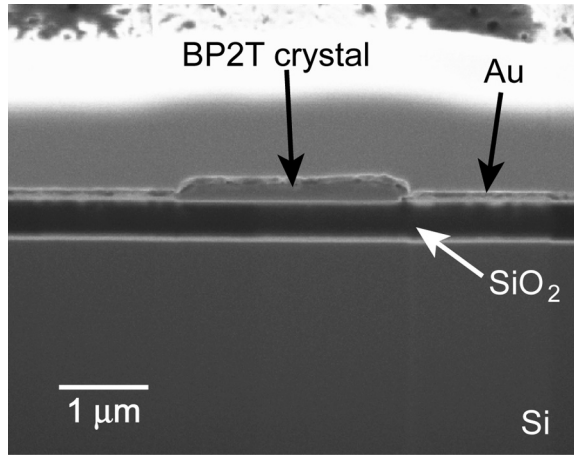

FIGURE 9 Cross section micrograph of the FET device of Figure 8. Copyright Wiley-VCH Verlag GmbH & Co. KGaA. Reproduced with permission from Ref. [13].

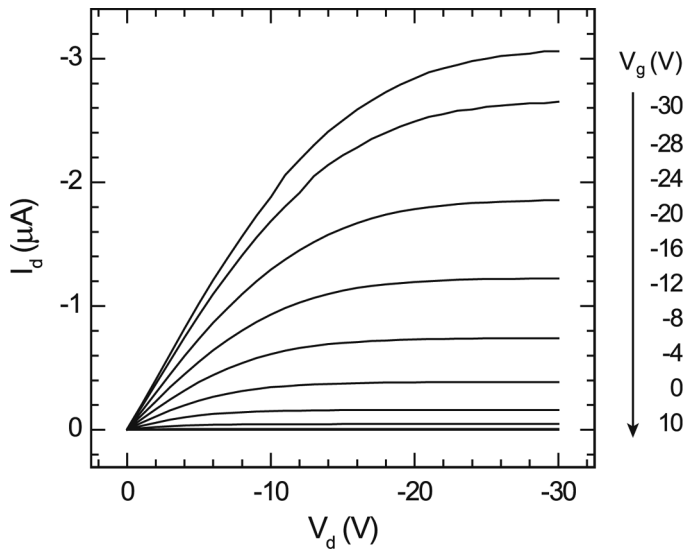

FIGURE 10 Drain current I_d vs. source-drain voltage V_d curves for various source-gate voltages V_g of the FET device (see Figures 8 and 9) at room temperature. I_d curves at V_g of 10 and 0 V nearly overlap. Copyright Wiley-VCH Verlag GmbH & Co. KGaA. Reproduced with permission from Ref. [13].

where L is the channel length, W_{eff} is the effective channel width, C_i is the capacitance (per unit area) of the insulator, and V_t is the threshold voltage. Ichikawa et al. estimated the mobility to be 0.66 cm^2/Vs. An excellent device performance is evident; individual characteristic curves stem from the origin and the drain-current saturation (pinch-off) is obviously noted. This mobility is comparable with that of high quality pentacene single crystals [16].

The needle crystals epitaxially grown on the KCl substrate are characterized by peculiar and interesting morphology. The molecules in the needles are arranged with their molecular long axes *perpendicular* to the needle long axis. The polarized emission observations clearly indicate that the molecules are deposited onto the KCl (001) surface such that their molecular long axes lie *parallel* to that surface [9]. These needle crystals give a unique opportunity to investigate the charge transport. This is because the face-to-face stacks of molecules developing along the needle naturally form a conduction path. Yanagi et al. [9] mention that the nonstraight TPCO molecules are good for forming well-defined needle crystals, partly because longer diffusion lengths of such molecules on the KCl surface allow them to migrate on the surface until being incorporated in the growing crystallites.

As another example we show a FET device directly grown in a liquid phase on the Si substrate. The top view of the device is depicted in Figure 11 [11]. Its device characteristics are given in Figure 12 [11]. A good device performance is again evident. The mobility estimated with Eq. 1 was 0.13–0.16 cm^2/Vs, depending upon the anisotropic electric measurements. In this case the aforementioned face-to-face stacks of the molecules form a conduction path in parallel with the substrate plane as well.

More recently even higher mobilities were recorded with single crystals of rubrene [17,18]. An upper limit of the mobility has to be pursued and determined with various organic materials having different morphologies, typically single crystals and thin films. A newly occurring class of organic devices are the light-emitting transistors (LETs). This was initially proposed by Hepp et al. [19]. Many researchers achieved the light emissions using thiophene-based oligomers on various FET device configurations [20–22]. These examples represent excellent integrations of the electronic and optical properties in a device.

PHOTONIC PROPERTIES

The TPCO flake crystals are suited for emission experiments. These crystals were irradiated with a pump laser beam and the resulting

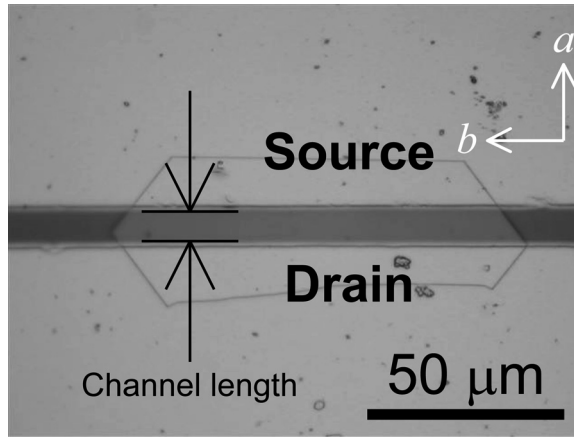

FIGURE 11 Micrograph of the FET device made of a BP3T thin crystal. The channel of the device was formed along the crystal *a*-axis. Yamao, T., Miki, T., Akagami, H., Nishimoto, Y., Ota, S., and Hotta, S., "Direct Formation of Thin Single Crystals of Organic Semiconductors onto a Substrate," *Chem. Mater.* **19**, 3748–3753 (2007). Reprinted with permission from Ref. [11]. Copyright 2007 American Chemical Society.

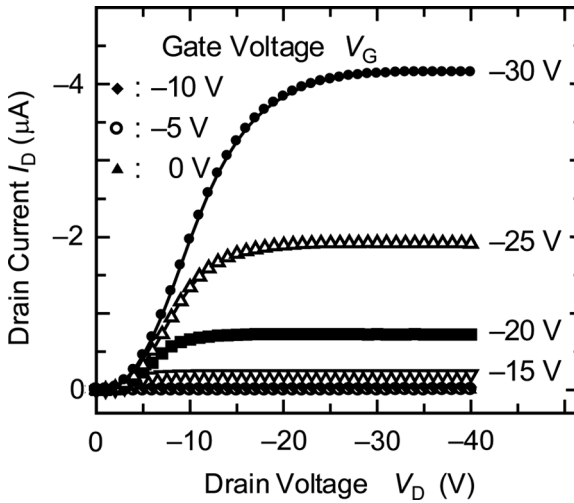

FIGURE 12 The characteristics of the BP3T FET device measured under an ambient environment. Reprinted with permission from Ref. [11]. Copyright 2007 American Chemical Society.

emissions that occurred from the crystal edges were collected and analyzed. When the intensity of the excitation laser beam is weak, the emissions exhibit broad spectra. On passing a certain threshold of excitation the emission spectra are suddenly narrowed. Such spectrally narrowed emissions (SNEs) reflect the high optical gain in the media. The SNEs include amplified spontaneous emission (ASE) [23–27], laser oscillation, and stimulated resonant Raman scattering [28].

Fichou et al. [23] and Horowitz et al. [24] first demonstrated the SNEs in single crystals of oligothiophenes. Nagawa et al. [25] and Shimizu et al. [26] also observed the SNE using a variety of TPCOs. They attributed the relevant SNE to the amplified spontaneous emission (ASE). So far, a variety of TPCOs have been found to show the SNE. In this context the unique crystallographic structures of TPCOs, especially the upright configuration of the molecular long axis, play an important role. This also causes the transition dipoles to stand upright against the bottom crystal face. As a result the intensity of emitted light is maximized in the direction parallel to the bottom crystal plane (i.e., the crystal faces of the thin flake crystals). This direction vertically penetrates a laterally spreading face-to-face array of molecules. What we expect from this molecular arrangement is that self-waveguided light propagating in the said direction can readily be amplified, producing a large optical gain along the bottom crystal plane. This explains well why the ASE takes place as edge emissions from the flake crystals [10b].

Very recently the laser oscillation has definitively been confirmed using TPCOs. Ichikawa et al. [29] and Shimizu et al. [30] observed the laser oscillation for single crystals of P6T and BP1T, respectively. In both cases the well-resolved and extremely narrow lines reflect the longitudinal cavity multimodes. The full width at half maximum (FWHM) of those lines was less than 0.1 nm.

The single crystals of P6T were grown in a gas phase [7,29]. The P6T crystals were formed as thin rectangular slabs (typically $\sim$3–10 mm long, 0.5–1 mm wide, and 1–3 μm thick) in a sealed glass tube filled with inert gas (argon). The crucial point is that the vertical crystal faces (i.e., the *ac*-plane) on either crystal edge form a pair of Fabry-Pérot cavities of optically high flatness. This ensures strong self-cavity optical confinement in the crystals. The optical resonator length is defined as the separation between the two ends (measured along the *b*-axis). These features agree with the statement by Karl [31] that the crystal used must be of "laser quality." In this respect the P6T undoped single crystals are supplied with the laser quality facets that act as the resonator, as in the case of the fluorine crystals doped with anthracene [31].

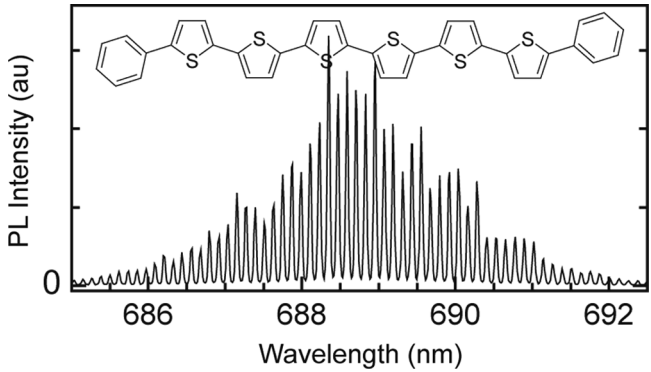

FIGURE 13 Emission spectrum of the laser oscillation of the P6T single crystal. Ichikawa, M., Hibino, R., Inoue, M., Haritani, T., Hotta, S., Araki, K., Koyama, T., and Taniguchi, Y., "Laser oscillation in monolithic molecular single crystals," *Adv. Mater.*, **17**(17), 2073–2077 (2005). Copyright Wiley-VCH Verlag GmbH & Co. KGaA. Reproduced with permission from Ref. [29].

The laser emission spectrum is shown in Figure 13 [29]. A progression of extremely narrow emission lines clearly appears around 689 nm. The FWHM of the individual lines is limited to 38 pm (close to the apparatus resolution limit). These narrow lines arise regularly at an interval of 121 pm. Figure 14 [29] shows the photopump intensity

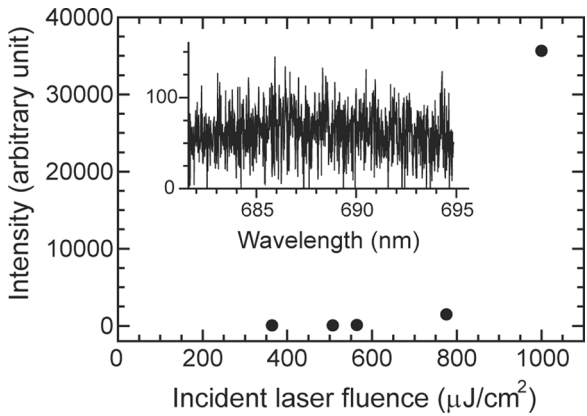

FIGURE 14 Photopumping intensity dependence of peak intensities of emission spectra from the P6T crystal. The data are indicated with closed circles. The inset depicts a spectrum taken with a fluence of 570 $\mu J/cm^2$. Copyright Wiley-VCH Verlag GmbH & Co. KGaA. Reproduced with permission from Ref. [29].

dependence of the peak intensities of the emission spectra. A threshold is clearly noted at $\sim 750\,\mu J/cm^2$. Concomitantly, the spectroscopic profiles dramatically change below and above the threshold (compare Figure 13 and the inset of Figure 14). Below the threshold, the emission spectra were weak and featureless, reflecting a nature of a spontaneous emission.

We present another example of the laser oscillation in the BP1T single crystals. To demonstrate this Shimizu et al. [30] carefully chose different hexagon single crystals of BP1T (0.56–1.06 mm long, ~ 0.15 mm wide, and $\sim 10\,\mu m$ thick). The line-shaped rectangular beam was incident vertical to the crystal face with the beam long axis parallel to the direction of the crystal long axis. The polarization direction of the linearly polarized laser beam was rotated by using a half wave plate in the direction either perpendicular or parallel to the crystal long axis.

Figure 15 [30] shows the spectral linewidth (FWHM) as a function of the excitation fluence for various excitation beam widths as parameters. When the beam width was 43 or 73 μm, the spectral width gradually decreased beyond the threshold with increasing excitation

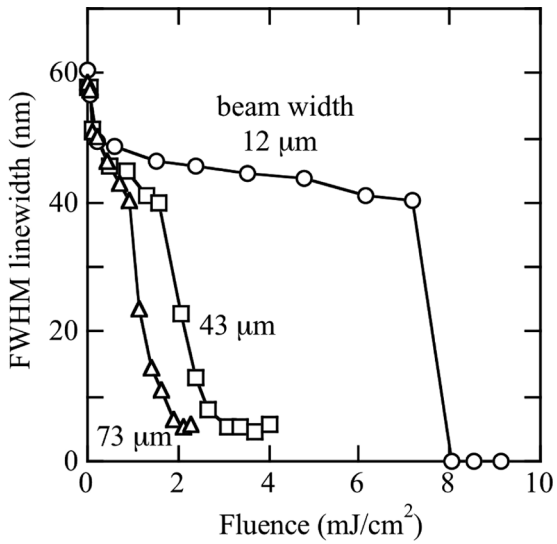

FIGURE 15 Spectral line widths (FWHM) as a function of the excitation fluence for various widths of the excitation beam. Shimizu, K., Mori, Y., and Hotta, S., "Laser oscillation from hexagonal crystals of a thiophene/phenylene co-oligomer," *J. Appl. Phys.*, **99**(6), 063505 (2006). Reprinted with permission from Ref. [30]. Copyright 2006, American Institute of Physics.

fluence and became constant ($\sim$5 nm). On the other hand, when the beam width was 12 μm, the emission linewidth suddenly decreased to $\sim$0.1 nm around a threshold fluence of 8 mJ/cm^2. Note that this threshold fluence is much larger than those observed for the 43- and 73-μm width excitations, which caused the ASE [23–27]. Nonetheless, once the laser oscillation sets in, the emission linewidths become by far narrower than those of the ASE. The sudden and abrupt onset of the spectral narrowing is also characteristic of the narrow line excitation ($\sim$10 μm width).

Figure 16 [30] shows the dependence of the emission spectra on the rotated angles of the half wave plate, which changed the polarization of the excitation laser beam. The rotated wave plate angles of 0° (90°) and 45° correspond to the polarization in the direction perpendicular and parallel to the crystal long axis, respectively. The data were collected using a crystal of 0.72 mm in length. The emission intensity

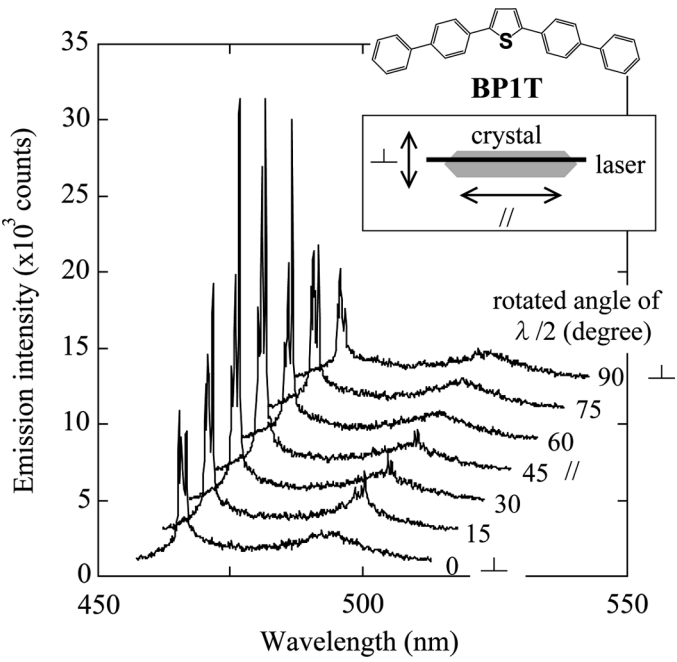

FIGURE 16 The dependence of the emission spectra on the polarization of the excitation laser beam. The inset represents that polarization either perpendicular (⊥) or parallel (//) to the molecular long axis. The beam width was 20 μm. Reprinted with permission from Ref. [30]. Copyright 2006, American Institute of Physics.

of the parallel polarization is 3.8 times as large as the perpendicular polarization.

CONCLUSION

We have developed a series of TPCOs by various organic syntheses. The syntheses were based mostly upon the Grignard coupling, Suzuki coupling, and Negishi coupling. The TPCOs systematically produce various molecular shapes by suitably arranging the thiophene and phenylene moieties. These materials were formed into crystals in a gas or liquid phase. These crystals have different morphologies (i.e., the flakes and needles) depending upon the difference in the crystal growth methods. The crystal structure is characterized by a "herringbone" structure that laterally spreads parallel to the bottom crystal plane. The strong face-to-face π-π interaction among the molecules is responsible for this structure. A further feature is that the molecular long axes stand upright against the bottom crystal plane.

We studied the charge transport and emission characteristics of the TPCO crystals. We measured their transport properties on the FET configurations. In both the needle crystals and flake crystals the face-to-face stacks of molecules naturally form the conduction paths, ensuring a good device performance. The maximum mobility has reached $\sim 1\,\mathrm{cm}^2/\mathrm{Vs}$ for the needle crystals of BP2T. To demonstrate the peculiar emission features of the TPCOs, we displayed the laser oscillation of the P6T and BP1T crystals. These illustrations are the first evidence of the laser oscillation in organic single crystals.

Once unique and promising electronic and photonic features have definitively been established, the TPCO materials and their optoelectronic device applications are expected to open up new routes to next-generation research and development of materials science.

REFERENCES

[1] Hotta, S. and Waragai, K., *Adv. Mater.* **5**, 896 (1993).
[2] Era, M., Tsutsui, T., and Saito, S., *Appl. Phys. Lett.* **67**, 2436 (1995).
[3] (a) Hotta, S., Lee, S. A., and Tamaki, T., *J. Heterocyclic Chem.* **37**, 25 (2000). (b) Hotta, S., Kimura, H., Lee, S. A., and Tamaki, T., *J. Heterocyclic Chem.* **37**, 281 (2000). (c) Hotta, S., *J. Heterocyclic Chem.* **38**, 923 (2001). (d) Hotta, S. and Katagiri, T., *J. Heterocyclic Chem.* **40**, 845 (2003). (e) Katagiri, T., Ota, S., Ohira, T., Yamao, T., and Hotta, S., *J. Heterocyclic Chem.* **44**, 853 (2007).
[4] Tamao, K., Kodama, S., Nakajima, I., Kumada, M., Minato, A., and Suzuki, K., *Tetrahedron* **38**, 3347 (1982).
[5] Miyaura, N. and Suzuki, A., *Chem. Rev.* **95**, 2457 (1995).
[6] Negishi, E.-I., Luo, F.-T., Frisbee, R., and Matsushita, H., *Heterocycles* **18**, 117 (1982).

[7] Ichikawa, M., Hibino, R., Inoue, M., Haritani, T., Hotta, S., Koyama, T., and Taniguchi, Y., *Adv. Mater*. **15**, 213 (2003).
[8] Yamao, T., Kawasaki, Y., Ota, S., Hotta, S., and Azumi, R., *Macromol. Symp*. **242**, 315 (2006).
[9] (a) Yanagi, H., Morikawa, T., Hotta, S., and Yase, K., *Adv. Mater*. **13**, 313 (2001). (b) Yanagi, H., Araki, Y., Ohara, T., Hotta, S., Ichikawa, M., and Taniguchi, Y., *Adv. Funct. Mater*. **13**, 767 (2003).
[10] (a) Hotta, S. and Goto, M., *Adv. Mater*. **14**, 498 (2002). (b) Hotta, S., Goto, M., Azumi, R., Inoue, M., Ichikawa, M., and Taniguchi, Y., *Chem. Mater*. **16**, 237 (2004). (c) Hotta, S., Goto, M., and Azumi, R., *Chem. Lett*. **36**, 270 (2007).
[11] Yamao, T., Miki, T., Akagami, H., Nishimoto, Y., Ota, S., and Hotta, S., *Chem. Mater*. **19**, 3748 (2007).
[12] Bernstein, J. and Sarma, J. A. R. P., *Chem. Phys. Lett*. **174**, 361 (1990).
[13] Ichikawa, M., Yanagi, H., Shimizu, Y., Hotta, S., Suganuma, N., Koyama, T., and Taniguchi, Y., *Adv. Mater*. **14**, 1272 (2002).
[14] Toda, Y. and Yanagi, H., *Appl. Phys. Lett*. **69**, 2315 (1996).
[15] Sze, S. M. (1981). *Physics of Semiconductor Devices*, John Wiley & Sons, Inc., New York, Chapter 8.
[16] Lee, J. Y., Roth, S., and Park, Y. W., *Appl. Phys. Lett*. **88**, 252106 (2006).
[17] Sundar, V. C., Zaumseil, J., Podzorov, V., Menard, E., Willett, R. L., Someya, T., Gershenson, M. E., and Rogers, J. A., *Science* **303**, 1644 (2004).
[18] Takeya, J., Yamagishi, M., Tominari, Y., Hirahara, R., Nakazawa, Y., Nishikawa, T., Kawase, T., Shimoda, T., and Ogawa, S., *Appl. Phys. Lett*. **90**, 102120 (2007).
[19] Hepp, A., Heil, H., Weise, W., Ahles, M., Schmechel, R., and von Seggern, H., *Phys. Rev. Lett*. **91**, 157406 (2003).
[20] Rost, C., Karg, S., Riess, W., Loi, M. A., Murgia, M., and Muccini, M., *Appl. Phys. Lett*. **85**, 1613 (2004).
[21] Oyamada, T., Sasabe, H., Adachi, C., Okuyama, S., Shimoji, N., and Matsushige, K., *Appl. Phys. Lett*. **86**, 093505 (2005).
[22] Yamane, K., Yanagi, H., Sawamoto, A., and Hotta, S., *Appl. Phys. Lett*. **90**, 162108 (2007).
[23] Fichou, D., Delysse, S., and Nunzi, J.-M., *Adv. Mater*. **9**, 1178 (1997).
[24] Horowitz, G., Valat, P., Garnier, F., Kouki, F., and Wintgens, V., *Opt. Mater*. **9**, 46 (1998).
[25] Nagawa, M., Hibino, R., Hotta, S., Yanagi, H., Ichikawa, M., Koyama, T., and Taniguchi, Y., *Appl. Phys. Lett*. **80**, 544 (2002).
[26] Shimizu, K., Hoshino, D., and Hotta, S., *Appl. Phys. Lett*. **83**, 4494 (2003).
[27] Xie, W., Li, Y., Li, F., Shen, F., and Ma, Y., *Appl. Phys. Lett*. **90**, 141110 (2007).
[28] Yanagi, H., Yoshiki, A., Hotta, S., and Kobayashi, S., *Appl. Phys. Lett*. **83**, 1941 (2003).
[29] Ichikawa, M., Hibino, R., Inoue, M., Haritani, T., Hotta, S., Koyama, T., and Taniguchi, Y., *Adv. Mater*. **15**, 213 (2003).
[30] Shimizu, K., Mori, Y., and Hotta, S., *J. Appl. Phys*. **99**, 063505 (2006).
[31] Karl, N., *Phys. Status Solidi A* **13**, 651 (1972).